

Sb₂O₂VO₃ as a candidate for an ideal inorganic spin-Peierls compound

I. Chaplygin

Institut für Physik, Technische Universität Chemnitz, D-09107 Chemnitz, Germany

R. Hayn

Leibniz-Institut für Festkörper- und Werkstofforschung (IFW) Dresden, P.O.Box 270016, D-01171 Dresden, Germany

(Received 6 May 2004; published 24 August 2004)

Band-structure calculations in the local spin-density approximation for the vanadium oxide Sb₂O₂VO₃ have been performed to estimate its hopping and exchange parameters. Comparing it with other one-dimensional cuprates and vanadates, we find Sb₂O₂VO₃ to be one of the most ideal inorganic spin-1/2 chain compounds synthesized so far. In connection with the observed spin gap, our results suggest Sb₂O₂VO₃ to be an ideal spin-Peierls compound, with a 25 times smaller exchange interchain coupling and a four times smaller frustration than in CuGeO₃.

DOI: 10.1103/PhysRevB.70.064510

PACS number(s): 75.10.Pq, 75.30.Et, 75.50.Ee

It was theoretically predicted that an ideal one-dimensional spin-1/2 chain compound should have a dimerized spin-Peierls ground state¹ due to the spin-lattice interaction. That is in close analogy to the instability of a one-dimensional metal by the Peierls effect.² The first observations of spin-Peierls transitions were achieved in organic materials.^{3,4} Recently, a major breakthrough in the field was reached by the discovery of the first inorganic spin-Peierls compound CuGeO₃,⁵ which allowed experiments with incomparable accuracy. However, detailed band-structure calculations revealed^{6,7} that CuGeO₃ is far from an ideal one-dimensional compound, having appreciable interchain couplings. In fact, the spin-Peierls transition in CuGeO₃ is more driven by the magnetic intrachain frustration (the exchange J' to second neighbors) than by the spin-lattice interaction. Indeed, it is known that a ratio J'/J (where J is the nearest-neighbor exchange) that exceeds the critical value of 0.241 (Ref. 8) already leads to a spin gap without any spin-lattice interaction, and CuGeO₃ is believed to have parameters close to that value.^{9,10}

The absence of a pseudogap above the transition temperature is another sign that CuGeO₃ does not behave like a classical spin-Peierls system.¹¹ It might be caused by the frustration discussed above, which makes the lattice dimerization of secondary importance. Another scenario is based on hard phonons and a strong spin-phonon coupling.¹² They bring about that CuGeO₃ is in the nonadiabatic limit,¹³ which means that the order parameter fluctuations are too fast to lead to a pseudogap.

It is therefore no surprise that there is a great activity to look for alternative inorganic spin-Peierls compounds, especially among cuprates or vanadates. However, up to now these attempts were not successful: the transition in NaV₂O₅ turned finally out to be due to charge ordering,¹⁴ and many one-dimensional compounds like MgVO₃ (Ref. 15) or CuSiO₃ (Ref. 16) have an antiferromagnetic (AF) instead of a dimerized ground state. In that respect, the observation of a spin gap in Sb₂O₂VO₃ (Ref. 17) is of great importance, despite the fact that up to now no lattice dimerization could be seen in the available polycrystalline samples. Indications of a

pseudogap could also be observed. To decide whether the observed spin gap could be due to the spin-Peierls effect and whether Sb₂O₂VO₃ is close to an ideal one-dimensional compound, a detailed, quantitative knowledge of the interchain couplings is crucial. For that purpose, we analyze here its electronic structure by means of band-structure calculations in the local spin-density approximation (LSDA). As it was shown already for other one-dimensional compounds,^{18,19} such an analysis allows a reliable determination of the different exchange terms. Our results show clearly that Sb₂O₂VO₃ is a nearly ideal one-dimensional compound, a much better one-dimensional compound than any other known cuprate or vanadate.

The crystal structure of Sb₂O₂VO₃ was defined by Darriet *et al.*²⁰ and is shown in Fig. 1. The structure is base-centered monoclinic $C2/c$. The primitive unit cell contains two formula units, and the parameters of the Bravais unit cell are $a=18.03$ Å, $b=4.800$ Å, $c=5.497$ Å, and $\beta=94.58^\circ$. As in most vanadates with V⁴⁺ ions, each vanadium ion is chemically bonded to five oxygen ions forming VO₅ pyramids. The four basal oxygen ions (O_B) are almost equidistantly remote from the vanadium ion and form the almost planar and square base of the pyramid. The fifth apical oxygen ion (O_A) is situated much closer to the vanadium ion. The VO₅ pyramids are arranged in edge-sharing VO₃ chains running along the c direction. Along the a direction, the chains are sepa-

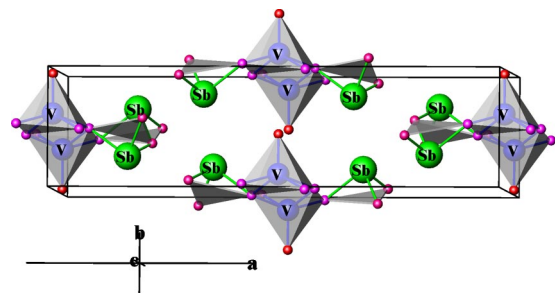


FIG. 1. (Color online) Polyhedral representation of the Sb₂O₂VO₃ crystal structure illustrating the chains of VO₅ pyramids. The small circles depict the oxygen ions.

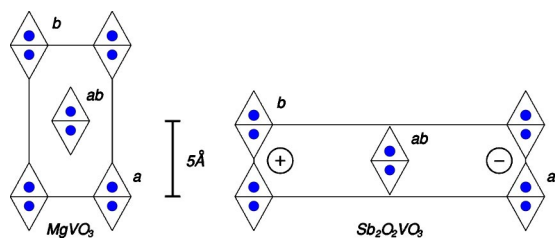


FIG. 2. (Color online) Schematic view of MgVO_3 and $\text{Sb}_2\text{O}_2\text{VO}_3$ along the chain direction c . Shown are the VO_5 pyramids with the central V ion (filled circles). The circled signs for $\text{Sb}_2\text{O}_2\text{VO}_3$ indicate the direction of shift along the c axis with respect to the central (ab) chain. The absolute value of the shift is about 0.72 \AA or 13% of the chain period. The upwards and downwards VO_5 pyramids alternate along the chain direction. The symbols a , ab , and b denote the neighboring chains (with respect to the chain in the lower left corner) in $(1,0,0)$, $(1/2,1/2,0)$, and $(0,1,0)$ crystallographic directions, respectively.

rated by doubled SbO layers. The chains are similar to those occurring in MgVO_3 as illustrated in Fig. 2. Some lattice parameters of the two compounds are compared in Table I.

The distance between the nearest chains in $\text{Sb}_2\text{O}_2\text{VO}_3$, $d_b=4.80 \text{ \AA}$, is shorter than $d_a=5.29 \text{ \AA}$ in MgVO_3 , which would suggest a larger interchain coupling. However, a closer inspection of the interchain arrangements (Fig. 2) shows a substantial difference: while in MgVO_3 the VO_5 pyramids of the nearest chains are connected by chemical bonds between the oxygen ions belonging to the base of the pyramids, in $\text{Sb}_2\text{O}_2\text{VO}_3$ it is the apical oxygen ion that is directed to the base of a pyramid in the nearest chain. That apical oxygen ion is strongly bond to the vanadium ion and does not participate in the electronic transfer. This, together with the fact that the other interchain distances in $\text{Sb}_2\text{O}_2\text{VO}_3$ are much larger than in MgVO_3 , results in the much more profound one-dimensional character of the first compound.

We have carried out scalar-relativistic calculations in LSDA for nonmagnetic (NM), ferromagnetic (FM), and antiferromagnetic (AF) structures of $\text{Sb}_2\text{O}_2\text{VO}_3$. The AF structure corresponds to alternating spins along the chain direction. We used the full-potential nonorthogonal local-orbital minimum-basis scheme²¹ and the basis set was chosen to be $\text{Sb } 4s4p4d5s5p$, $\text{V } 3s3p3d4s4p$, $\text{O } 2s2p3d$. Similar to MgVO_3 , the spin-polarized calculations give rise

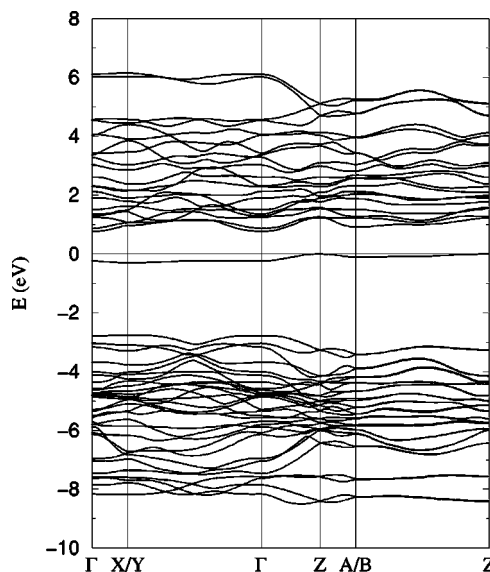


FIG. 3. The band structure for the antiferromagnetic solution.

to insulating magnetic solutions with the magnetic moment of vanadium ion and the insulating gap being about $1.024 \mu_B/0.52$ and $0.947 \mu_B/0.76 \text{ eV}$ for FM and AF solutions, respectively. Probably, the real gap is enhanced by correlation effects but it was not yet measured. The total energy of the AF solution is 14.2 meV per formula unit lower than that of the FM one. In the framework of the Heisenberg model

$$\hat{H} = \sum_i JS_i S_{i+1},$$

we compare it with the energy difference between the FM solution $E_F=J/4$ and the Néel state $E_A=-J/4$ and obtain $J=330 \text{ K}$. The quantum fluctuations lower the energy of the AF state, so that the difference $E_F-E_A=J \ln 2$ (Ref. 22) becomes larger. There is a great uncertainty how much quantum fluctuations are included into the LSDA solution, but the resulting estimate of $J=238 \text{ K}$ is in reasonable agreement with the experimental value $J=250 \text{ K}$.¹⁷

The band structure of all three solutions is qualitatively similar (besides the band near the Fermi level), and we show

TABLE I. Parameters characterizing the VO_3 chain structure. Distances are given in Å . O_A and O_B designate apical and basal oxygen ions, respectively. The “Next chain” section represents the distances between close ions in the *different* chains.

| | VO_5 pyramid | | | | Chain | |
|------------------------------------|-----------------------|-----------------|-----------------------------|-----------------------------|-----------------------------|-----------------------------|
| | V- O_A | V- O_B | O_A - O_B | O_B - O_B | V-V | V- \hat{V} -V |
| MgVO_3 | 1.63 | 1.95 | 2.95 | 2.53/2.62 | 2.96 | 124.5° |
| $\text{Sb}_2\text{O}_2\text{VO}_3$ | 1.59 | 1.91/2.04 | 2.78/3.00 | 2.57/2.77 | 3.01 | 132.2° |
| | Interchain | | | Next chain | | |
| | d_a | d_{ab} | d_b | O_B - O_B | O_A - O_B | O_A - O_A |
| MgVO_3 | 5.29 | 5.67 | 10.03 | 2.76 | ... | ... |
| $\text{Sb}_2\text{O}_2\text{VO}_3$ | 18.03 | 9.33 | 4.80 | ... | 3.12/3.28 | 2.78 |

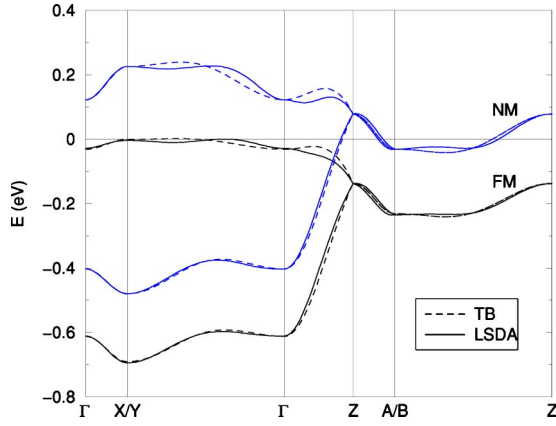


FIG. 4. (Color online) The bands crossing the Fermi level in the NM and the FM LSDA solutions and their TB fits.

in Fig. 3 that one corresponding to the AF ground state. According to our orbital analysis, the 30 bands between -9 and -3 eV are mainly built up of O $2p$ states. The band complex consisting of the highest occupied band and the conduction bands up to 7 eV (altogether 22 bands) are built up of the V $3d$ and the Sb $4p$ states. To perform the orbital analysis, we set the quantization axis z along the b direction (the direction of the bond between vanadium and apical oxygen ions) and the axis y along the chain direction c .

As in MgVO₃ the lowest V $3d$ state appears to be of mostly $d_{x^2-y^2}$ character and well separated from the rest of the electronic system. That situation, characteristic for vanadates with V⁴⁺ ions, is different from the case of cuprates, in which the upper d_{xy} (Ref. 23) band is relevant. Consequently, the transition metal ion is bound to basal oxygens by $dp\pi$ bonds in vanadates, in contrast to the $dp\sigma$ bonds in cuprates.

In the NM metallic solution, a band with a width of about 0.7 eV crosses the Fermi level. The corresponding band of the FM solution is similar, only shifted below the Fermi level. Both bands are shown in Fig. 4 together with the corresponding tight-binding (TB) fits. The relevant band is split in the AF case, due to the alternation of on-site energies, which makes a TB fit more involved but does not provide principally new information. One can see in Fig. 4 that the band has much smaller dispersion in the direction connecting the nearest chains (ΓY) than that of MgVO₃,¹⁸ especially for the lower part of the band, revealing more profound one-dimensional character than the latter compound.

To quantify the result, a TB analysis has been performed for the relevant band of the NM and the FM solutions. Hopping processes to the neighbors in the nearest chains, and to the nearest and the next-nearest neighbors in chain direction were taken into account. The lower index designates the di-

TABLE II. The TB parameters (in meV) corresponding to the NM and the FM band structure of Sb₂O₂VO₃.

| | t_c | t'_c | t_b | t_{bc} | t'_{bc} | t_{ab} | t_{abc} | t'_{abc} |
|----|-------|--------|-------|----------|-----------|----------|-----------|------------|
| NM | 152.7 | 25.8 | 0.9 | 0.6 | 6.8 | -6.0 | -5.6 | 3.8 |
| FM | 154.1 | 27.8 | -1.4 | 2.4 | 4.8 | -7.4 | -3.4 | 2.2 |

rection of the transfer process (c is the chain direction) and the prime signs two steps in c direction:

$$\begin{aligned}
 E_0 - E_{\mathbf{k}} = & 2t_c \cos k_c \frac{c}{2} + 2t'_c \cos k_c c + 2 \cos k_b b \left(t_b \right. \\
 & \left. + 2t_{bc} \cos k_c \frac{c}{2} + 2t'_{bc} \cos k_c c \right) \\
 & + 4 \cos k_a \frac{a}{2} \cos k_b \frac{b}{2} \left(t_{ab} + 2t_{abc} \cos k_c \frac{c}{2} \right. \\
 & \left. + 2t'_{abc} \cos k_c c \right),
 \end{aligned}$$

yielding the parameters which are collected in Table II.

The deviations between fit and band structure are smaller for the FM solution, probably due to larger hybridization with higher lying states in the NM case. In other respects, the differences are small, proving the reliability of our approach. t_c and t'_c are the in-chain hopping parameters to the nearest and next-nearest neighbor, from now on denoted by t and t' , respectively, and t_{\perp} is the largest out-of-chain hopping parameter. These TB parameters for Sb₂O₂VO₃ are compared in Table III with similar fits for some other one-dimensional compounds with spin-Peierls (CuGeO₃) or AF ground-state (MgVO₃, Sr₂CuO₃). Adding the Coulomb correlation U , one can estimate the exchange couplings from the TB parameters by $J_i = 4t_i^2/U$. Thus, the ratios of exchange parameters are roughly proportional to the square of the ratios of hopping values. One sees that t_{\perp}/t is 5 times smaller in Sb₂O₂VO₃ than in CuGeO₃ suggesting a 25 times smaller interchain exchange coupling, whereas t is roughly the same, in agreement with the similarity of the experimental values for the in-chain exchange couplings $J \approx 21$ and 14 meV for Sb₂O₂VO₃ (Ref. 17) and CuGeO₃,²⁴ respectively. In contrast, MgVO₃ shows such a large interchain coupling that it is better regarded as an anisotropic two-dimensional system. Furthermore, t'/t is two times smaller in Sb₂O₂VO₃ than in CuGeO₃ which indicates a four times smaller frustration. It is known that magnetic frustration can lead to a spin gap,²⁵ and can therefore be regarded as the second driving force towards the spin-Peierls transition besides the electron-lattice interaction. Taking into account the interchain couplings as third interaction one finds a competition between the AF and the spin-Peierls state. Large interchain couplings usually prefer the AF state, as can be seen in MgVO₃.²⁶ Therefore, the remarkable interchain couplings in CuGeO₃ lead us to con-

TABLE III. The TB parameters (in meV) for four one-dimensional compounds.

| | Sb ₂ O ₂ VO ₃ | CuGeO ₃ ^a | MgVO ₃ ^b | Sr ₂ CuO ₃ ^c |
|-------------|--|---------------------------------|--------------------------------|---|
| t | 154 | 175 | 160 | 550 |
| t' | 26 | 51 | 20 | 100 |
| t_{\perp} | 7 | 34 | 40 | 30 |

^aSee Ref. 7.

^bSee Ref. 18.

^cSee Ref. 19.

clude that its spin-Peierls transition is dominated by the magnetic frustration. On the other hand, due to the much smaller frustration in $\text{Sb}_2\text{O}_2\text{VO}_3$, its spin-Peierls effect should be more driven by magnetoelastic effects. To have a first idea, one can compare the VO_2 ribbons in $\text{Sb}_2\text{O}_2\text{VO}_3$ with the CuO_2 ribbons in CuGeO_3 that are plane in the high-temperature phase. There, the spin-Peierls distortion leads to nonplanar ribbons and to two crystallographic different oxygen positions.²⁷ One might speculate that the nonplanar ribbon geometry in $\text{Sb}_2\text{O}_2\text{VO}_3$ facilitates the spin-Peierls transition leading to two different oxygen positions as in CuGeO_3 . The presence of nonadiabatic effects and of a strong frustration in CuGeO_3 and its absence in $\text{Sb}_2\text{O}_2\text{VO}_3$ suggests also a crucial role of the frustration for the nonadiabaticity. On the contrary, $\text{Sb}_2\text{O}_2\text{VO}_3$ can be expected to be a much better model spin-Peierls system in the classical sense. The ratios of t_{\perp}/t and t'/t in $\text{Sb}_2\text{O}_2\text{VO}_3$ are of the same order than in the edge-sharing cuprate chain Sr_2CuO_3 being presently the best model compound for 1D spin-1/2 antiferromagnetism.¹⁹ However, the absolute values of t are very different, leading to a one-order of magnitude difference for J . That might be the reason for the different ground states in both compounds since the energy gain due to dimerization can be expected to be similar, whereas the magnetic order is much more favored in Sr_2CuO_3 .

Let us briefly discuss the reliability of our estimated exchange couplings. If the relevant band at the Fermi level is well isolated from other band complexes (see Fig. 3, which is also the case for all other compounds of Table III) its TB parameters (see Table II) correspond to the hopping between Wannier orbitals that are constructed of a $3d$ orbital and its hybridizations to the neighboring oxygen orbitals. These hopping terms are less influenced by the Coulomb correla-

tion and rather different approaches up to quantum chemical methods²⁸ give comparable values. The superexchange $J = 4t^2/U$ of these Wannier orbitals contains implicitly all the different exchange paths via intermediate oxygen orbitals. That explains why such an oversimplified expression may reproduce the correct chemical tendency between Sr_2CuO_3 and Ca_2CuO_3 .¹⁹ Possible corrections are due to ring exchange processes²⁹ or due to the direct FM exchange.³⁰ Whereas the former processes are usually very small, the latter should be discussed more in detail. The magnitude of the direct FM exchange is small for the interchain couplings, but it could be important if the AF superexchange is suppressed, as shown recently for $\text{La}_4\text{Ba}_2\text{Cu}_2\text{O}_{14}$ with $t \sim 3 \text{ meV}$.³⁰ There, the sign of the exchange coupling changed, but the order of magnitude remained correct. The absolute value of direct exchange might be larger for the nearest-neighbor exchange,⁷ which reduces the nearest-neighbor exchange. In any case, the expression $4t_i^2/U$ should be considered as a rough estimate, which provides, however, the correct order of magnitude and the correct chemical trends.

To conclude, we estimated the interchain couplings by band-structure calculations and found $\text{Sb}_2\text{O}_2\text{VO}_3$ to be one of the most ideal, inorganic, spin-1/2 chain compounds synthesized so far, more ideal than CuGeO_3 . The reason is a smaller interchain exchange coupling (by roughly a factor of 25) and a smaller frustration. Further experimental studies in addition to the sole demonstration of a spin gap,¹⁷ would be highly encouraged to investigate the spin-Peierls transition in its classical sense.

We thank A. Stepanov and S.-L. Drechsler for useful discussions.

-
- ¹D. B. Chesnut, *J. Chem. Phys.* **45**, 4677 (1966).
²R. E. Peierls, *Quantum Theory of Solids* (Clarendon, Oxford, 1955) p. 108.
³J. W. Bray, H. R. Hart, Jr., L. V. Interrante, I. S. Jacobs, J. S. Kasper, G. D. Watkins, S. H. Wee, and J. C. Bonner, *Phys. Rev. Lett.* **35**, 744 (1975).
⁴I. S. Jacobs, J. W. Bray, H. R. Hart, Jr., L. V. Interrante, J. S. Kasper, G. D. Watkins, D. E. Prober, and J. C. Bonner, *Phys. Rev. B* **14**, 3036 (1976).
⁵M. Hase, I. Terasaki, and K. Uchinokura, *Phys. Rev. Lett.* **70**, 3651 (1993).
⁶L. F. Mattheiss, *Phys. Rev. B* **49**, 14 050 (1994).
⁷H. Rosner, S.-L. Drechsler, K. Koepernik, R. Hayn, and H. Eschrig, *Phys. Rev. B* **63**, 073104 (2001).
⁸K. Okamoto and K. Nomura, *Phys. Lett. A* **169**, 433 (1992).
⁹G. Castilla, S. Chakravarty, and V. J. Emery, *Phys. Rev. Lett.* **75**, 1823 (1995).
¹⁰J. Riera and A. Dobry, *Phys. Rev. B* **51**, 16 098 (1995).
¹¹P. A. Lee, T. M. Rice, and P. W. Anderson, *Phys. Rev. Lett.* **31**, 462 (1973).
¹²C. Gros and R. Werner, *Phys. Rev. B* **58**, R14 677 (1998).
¹³G. Wellein, H. Fehske, and A. P. Kampf, *Phys. Rev. Lett.* **81**, 3956 (1998).
¹⁴A. N. Yaresko, V. N. Antonov, H. Eschrig, P. Thalmeier, and P. Fulde, *Phys. Rev. B* **62**, 15 538 (2000).
¹⁵J. Choukroun, V. A. Pashchenko, Y. Ksari, J. Y. Henry, F. Mila, P. Millet, P. Monod, A. Stepanov, J. Dumas, and R. Buder, *Eur. Phys. J. B* **14**, 655 (2000).
¹⁶M. Baenitz, C. Geibel, M. Dischner, G. Sparr, F. Steglich, H. H. Otto, M. Meibohm, and A. A. Gippius, *Phys. Rev. B* **62**, 12 201 (2000).
¹⁷V. A. Pashchenko, A. Sulpice, F. Mila, P. Millet, A. Stepanov, and P. Wyder, *Eur. Phys. J. B* **21**, 473 (2001).
¹⁸I. Chaplygin, R. Hayn, and K. Koepernik, *Phys. Rev. B* **60**, R12 557 (1999).
¹⁹H. Rosner, H. Eschrig, R. Hayn, S.-L. Drechsler, and J. Málek, *Phys. Rev. B* **56**, 3402 (1997).
²⁰B. Darriet, J. Bovin, and J. Galy, *J. Solid State Chem.* **19**, 205 (1976).
²¹K. Koepernik and H. Eschrig, *Phys. Rev. B* **59**, 1743 (1999).
²²L. Hulthén, *Ark. Mat., Astron. Fys.* **26A**, 1 (1938).
²³Note that our coordinate system is rotated by 45° with respect to the one standardly used for the CuO_4 plaquette, where the axes are directed along the Cu-O bonds.

- ²⁴K. Fabricius, A. Klümper, U. Löw, B. Büchner, T. Lorenz, G. Dhaleene, and A. Revcolevschi, *Phys. Rev. B* **57**, 1102 (1998).
- ²⁵C. K. Majumdar and D. K. Ghosh, *J. Math. Phys.* **10**, 1388 (1969).
- ²⁶Even if the spin-Peierls state is realized, small but finite inter-chain couplings are necessary to explain a finite transition temperature.
- ²⁷M. Braden, G. Wilkendorf, J. Lorenzana, M. Ain, G. J. McIntyre, M. Behruzi, G. Heger, G. Dhahenne, and A. Revcolevschi, *Phys. Rev. B* **54**, 1105 (1996).
- ²⁸C. de Graaf, I. de P. R. Moreira, F. Illas, O. Iglesias, and A. Labarta, *Phys. Rev. B* **66**, 014448 (2002).
- ²⁹S. Feldkemper, W. Weber, J. Schulenburg, and J. Richter, *Phys. Rev. B* **52**, 313 (1995).
- ³⁰W. Ku, H. Rosner, W. E. Pickett, and R. T. Scalettar, *Phys. Rev. Lett.* **89**, 167204 (2002).